Available online at www.sciencedirect.com

SCIENCE DIRECT

Developmental Biology 283 (2005) 373 – 383

DEVELOPMENTAL BIOLOGY

www.elsevier.com/locate/ydbio

Differential roles of $p39^{Mos}$–$Xp42^{Mpk1}$ cascade proteins on Raf1 phosphorylation and spindle morphogenesis in *Xenopus* oocytes

J.-F.L. Bodart[a,*,1], F.Y. Baert[a,1], C. Sellier[a], N.S. Duesbery[b], S. Flament[c], J.-P. Vilain[a]

[a]*Laboratoire de Biologie du Développement, UPRES EA 1033, Université des Sciences et Technologies de Lille, SN3, F-59655 Villeneuve d'Ascq CEDEX, France*

[b]*Laboratory of Cancer and Developmental Cell Biology, Van Andel Research Institute, Grand Rapids, MI 49503, USA*

[c]*Faculté des Sciences, EA 3442, Génétique, Signalisation, Différenciation, Université Henri Poincaré, entrée 1B, 9ème étage, Boulevard des Aiguillettes, BP239, 54506, Vandoeuvre lez Nancy CEDEX, France*

Received for publication 16 December 2004, revised 12 April 2005, accepted 15 April 2005
Available online 23 May 2005

Abstract

Fully-grown G2-arrested *Xenopus* oocytes resume meiosis upon hormonal stimulation. Resumption of meiosis is characterized by germinal vesicle breakdown, chromosome condensation, and organization of a bipolar spindle. These cytological events are accompanied by activation of MPF and the $p39^{Mos}$–MEK1–$Xp42^{Mpk1}$–$p90^{Rsk}$ pathways. The latter cascade is activated upon $p39^{Mos}$ accumulation. Using U0126, a MEK1 inhibitor, and $p39^{Mos}$ antisense morpholino and phosphorothioate oligonucleotides, we have investigated the role of the members of the $p39^{Mos}$–MEK1–$Xp42^{Mpk1}$–$p90^{Rsk}$ in spindle morphogenesis. First, we have observed at a molecular level that prevention of $p39^{Mos}$ accumulation always led to MEK1 phosphorylation defects, even when meiosis was stimulated through the insulin Ras-dependent pathway. Moreover, we have observed that Raf1 phosphorylation that occurs during meiosis resumption was dependent upon the activity of MEK1 or $Xp42^{Mpk1}$ but not $p90^{Rsk}$. Second, inhibition of either $p39^{Mos}$ accumulation or MEK1 inhibition led to the formation of a cytoplasmic aster-like structure that was associated with condensed chromosomes. Spindle morphogenesis rescue experiments using constitutively active Rsk and purified murine Mos protein suggested that $p39^{Mos}$ or $p90^{Rsk}$ alone failed to promote meiotic spindle organization. Our results indicate that activation of the $p39^{Mos}$–MEK1–$Xp42^{Mpk1}$–$p90^{Rsk}$ pathway is required for bipolar organization of the meiotic spindle at the cortex.

Keywords: Spindle formation; $p39^{Mos}$; MAP Kinase; Meiosis; *Xenopus*

Introduction

Fully-grown *Xenopus laevis* oocytes are arrested at prophase of the first meiotic division. In response to stimulation by steroid hormones, they resume meiosis in a process called maturation. Release from prophase I-arrest is analogous to G2/M transition, and is characterized by the movement of the nucleus or germinal vesicle (GV) towards the animal cortex, breakdown of the nuclear envelope (germinal vesicle breakdown or GVBD), chromosome condensation, and the formation of a bipolar spindle. Anchoring of the spindle at the cortex is accompanied by the appearance of a white spot (WS) at the apex of the oocyte. The first meiotic division is completed after extrusion of the first polar body. The second division resumes in absence of interphase and arrests at metaphase II in preparation for fertilization (Hausen and Riebesell, 1991).

The molecular mechanisms underlying the morphogenesis of the first meiotic spindle are poorly characterized. Unlike mitosis, first meiotic spindle formation in *Xenopus* oocytes proceeds in absence of active centrosomes. Indeed, centrosomes are functionally inactivated at earlier stages of oogenesis (Gard et al., 1995).

* Corresponding author. Fax: +33 32043 4038.
E-mail address: Jean-Francois.bodart@univ-lille1.fr (J.-F.L. Bodart).
[1] Co-authors.

0012-1606/$ - see front matter © 2005 Elsevier Inc. All rights reserved.
doi:10.1016/j.ydbio.2005.04.031

Cytological events of maturation are triggered by the activation of protein kinase signaling pathways culminating with the activation of M-phase promoting factor (MPF), a cytoplasmic protein complex that controls G2/M transition. MPF is a heterodimer made up of two subunits: a catalytic subunit, the kinase $p34^{Cdc2/Cdk1}$, and a regulatory subunit, the cyclin B (for review, see Masui, 2001; Nurse et al., 1998). At the same time, $Xp42^{Mpk1}$ is phosphorylated and activated (Ferrell et al., 1991). $Xp42^{Mpk1}$ is a mitogen-activated protein kinase (MAPK) that is turned on following progesterone-induced synthesis of $p39^{Mos}$ (a mitogen-activated protein kinase kinase kinase) and subsequent phosphorylation of mitogen-activated protein kinase kinase 1 (MEK1) (Nebreda and Hunt, 1993; Sagata et al., 1988). $Xp42^{Mpk1}$ in turn phosphorylates and activates ribosomal S6 kinase ($p90^{Rsk}$). Accumulation of $p39^{Mos}$ can either be controlled by $Xp42^{Mpk1}$ through the regulation of $p39^{Mos}$ mRNA translation (Howard et al., 1999) or by MPF-dependent mechanisms (Frank-Vaillant et al., 1999). Activity of the $p39^{Mos}$–$Xp42^{Mpk1}$ pathway is not required in *Xenopus* oocytes (Bodart et al., 2002; Fisher et al., 1999; Gross et al., 2000). However, this pathway has been shown to be responsible for S-Phase suppression between meiosis I and meiosis II; inhibition of $p39^{Mos}$ synthesis (Dupre et al., 2002; Furuno et al., 1994) or inhibition of MEK1 activity (Gross et al., 2000) prevents meiosis I–meiosis II transition and allows inappropriate DNA replication.

Available evidence indicates that the MAPK pathway is involved in spindle formation and stabilization. In mouse oocytes, MAPK has been found to be associated with MTOC (Verlhac et al., 1994). In mouse and pig oocytes, MAPK distributes to the metaphase spindle and migrates to the middle of the spindle during the transition from anaphase to telophase (Hatch and Capco, 2001; Lee et al., 2000). The same pattern of distribution has been observed for its downstream effector, $p90^{Rsk}$ (Fan et al., 2003). Interestingly, amphibian and mammalian oocytes in which the MAPK pathway is inactive fail to assemble a normal spindle (Araki et al., 1996; Bodart et al., 2002; Choi et al., 1996; Zhao et al., 1991). Phosphorylation of two MAP kinase substrates is required for normal meiotic spindle morphogenesis in mouse oocytes (Lefebvre et al., 2002; Terret et al., 2003). However, mouse oocytes deficient in MAP kinase activity can still divide and release polar body. In this case, the polar body is abnormally large (Verlhac et al., 2000).

This study was undertaken to analyze in vivo the effects of $p39^{Mos}$–$Xp42^{Mpk1}$ pathway on meiotic spindle. Both chemical inhibitor and antisense strategies were used and their effects on the MAP kinase cascade regulation as well as on the MEK kinase Raf1 have been analyzed and discussed. Our results provide evidences that $p39^{Mos}$ is the only MAPKK kinase involved in MEK1 phosphorylation and that Raf complete phosphorylation is dependent upon phosphorylation by either MEK1 or Xp42Mpk1. While inactivation of MAP kinase leads to formation of aster-like structures, we observed that members of $p39^{Mos}$–$Xp42^{Mpk1}$ pathway might play complementary but different roles in spindle formation.

Materials and methods

Isolation of oocytes

Adult *Xenopus* females were purchased from University of Rennes I, France. After anesthetizing frogs by immersion in 1 g/l MS222 solution (tricaine methane sulfonate, Sandoz), ovarian lobes were surgically removed and placed in ND96 medium [96 mM NaCl, 2 mM KCl, 1.8 mM $CaCl_2$, 1 mM $MgCl_2$, 5 mM HEPES, pH 7.5 (NaOH)]. Fully-grown stage VI oocytes (Dumont, 1972) were isolated and defolliculated by partial collagenase treatment for 30 min (1 mg/ml collagenase A, Roche), followed by manual microdissection. Oocytes were stored at 14°C in ND96 medium prior to use. All treatments were started within 24 h of ovarectomies.

Antisense oligonucleotides

Phosphorothioate deoxyribo-oligonucleotides were purchased from Eurogentec. The sequence of the antisense against $p39^{Mos}$ was AAGGCATTGCTGTGTGACTCGCTGAAAC and was similar to those described in Sagata et al. (1988). As control, we used the inverted sequence GTTTCAGCGAGTCACACAGCAATGCCTT designed as sense oligonucleotides or RNase free water.

Morpholino oligonucleotides were purchased from Gene Tools. The sequence of the antisense against $p39^{Mos}$ was GGGAAGGCATTGCTGTGTGACTCGC. As a control, we used the inverted sequence CGCTCAGTGTGTCGTTACGGAAGGG and also a standard sense control CCTCTTACCTCAGTTACAATTTATA.

For both phosphorothioate and morpholino oligonucleotides, 1 ng was microinjected into each oocyte by the use of a positive displacement digital micropipette (Nichiryo). Oocytes were then incubated in ND96 medium for progesterone experiments and in OR-2 medium for insulin experiments (see Baert et al., 2003). U0126 (Promega) was prepared in DMSO and used at a final concentration of 10 to 50 μM. Treatments began 1 h before progesterone or insulin addition. Control oocytes were treated with an identical amount of DMSO (0.2‰ to 1‰).

Oocyte treatments

Purified murine Mos protein (Mu-Mos) was kindly provided by Dr. Vande Woude. Purified constitutively active Rsk (CA-Rsk) was a gift of Dr. Nebreda (Perdiguero et al., 2003). Mu-Mos (37.5 ng) and CA-Rsk (5 ng) were injected into each oocytes (in a volume of 50 nl) just prior to progesterone or insulin treatment.

Resumption of meiosis was stimulated by incubating oocytes in ND96 medium containing 10 μM progesterone (Sigma). Incubation in DMSO (1‰) or injection with PSS (Phosphorothioate Sense oligonucleotide) was used as controls for U0126 and PSAS (Phosphorothioate Antisense oligonucleotide) experiments, respectively. Batches of injected oocytes (30 to 60) from different females (n = number of animals) were observed every hour and scored for the appearance of white spot. Experiments were ended 2 h after stabilization of white-spot percentage (10 to 14 h after first white-spot appearance). Three to 5 oocytes were frozen at −20°C for later biochemical analysis and the rest of the oocytes were fixed for cytological analysis (see below).

Cytological and immunocytological analysis

For classical cytological analysis, oocytes were fixed overnight in Smith's fixative, dehydrated, and embedded in paraffin. Sections (7 μm thick) were stained with nuclear red to detect nuclei and chromosomes and with picroindigo carmine that reveals cytoplasmic structures.

For immunocytological analysis, oocytes were fixed overnight in cold methanol, which was gradually replaced by butanol before embedding in paraffin. 10-μm sections were cut and stained with 1 μg/ml Hoechst 33342 (Sigma) to visualize chromosomes. Microtubules were stained with monoclonal anti-tubulin antibody Tub 2.1 (Sigma). Primary antibodies were revealed with antimouse antibody coupled to Oregon Green (Molecular Probes).

Western blotting

Oocytes were lysed in homogenization buffer (Azzi et al., 1994) and then centrifuged for 5 min at 10,000×g (4°C) to eliminate yolk platelets. Proteins were then separated on a 12.5% mini-SDS-polyacrylamide gel for phospho-MEK immunodetection or on a modified 17.5% polyacrylamide gel for Raf, $p39^{Mos}$, $Xp42^{Mpk1}$, and $p90^{Rsk}$ immunodetection (Bodart et al., 1999). $Xp42^{Mpk1}$ was detected using the D-2 monoclonal antibody (Santa Cruz Biotechnology; 1/1000). $p39^{Mos}$ was detected using the C238 polyclonal antibody (Santa Cruz Biotechnology; 1/1000). $p90^{Rsk}$ detection was performed using the C21 polyclonal antibody (Santa Cruz Biotechnology; 1/1000). Raf was detected using the C20 polyclonal antibody (Santa Cruz Biotechnology; 1/500) and phospho-MEK detection was performed using a polyclonal antibody (Calbiochem; 1/1000). Signals were detected by using enhanced chemoluminescence (Amersham).

Statistical analysis

Statistical analyses of kinetic experiments were performed by a logrank test (survival test). Observed counts in cytological studies were compared using the chi-square analysis of contingency tables or the Fisher exact test if one or more values were equal to zero.

Results

Dose-dependent effects of MEK inhibition on G2/M transition

To analyze the impact of the inhibition of the $p39^{Mos}$–MEK1–$Xp42^{Mpk1}$–$p90^{Rsk}$ pathway on spindle morphogenesis, we determined the effects of two strategies on $Xp42^{Mpk1}$ activity and $p39^{Mos}$ accumulation.

Dose-dependent effects of the MEK inhibitor U0126 on meiotic resumption induced by progesterone or insulin were first investigated. Previous observations reported by Gross et al. (2000) indicated that 50 μM U0126 did not block progesterone-induced GVBD but rather delayed it. Using increasing concentration of U0126 (10 to 50 μM) on progesterone-stimulated oocytes, we similarly observed that U0126 never prevented GVBD though it did delay GVBD (Fig. 1A). Even at 100 μM, U0126 did not prevent GVBD (data not shown). In oocytes treated by U0126 10 μM, time of $GVBD_{50}$ (time to which 50% of the oocytes underwent

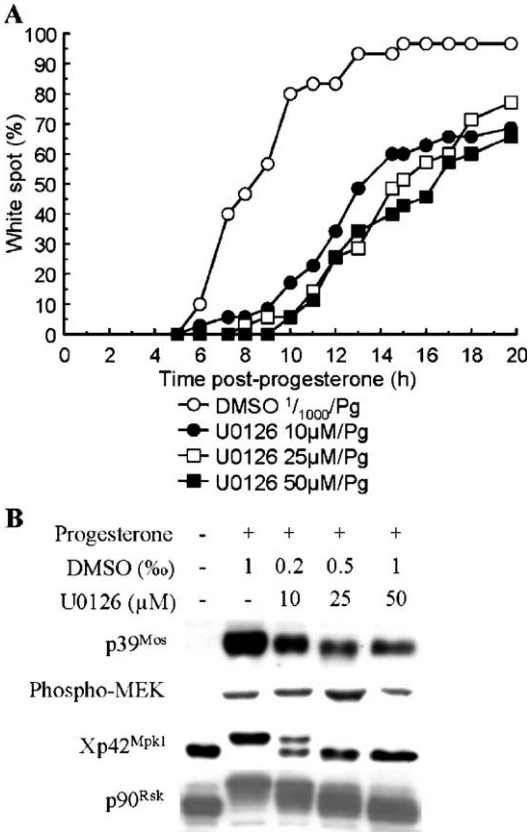

Fig. 1. Dose-dependent effects of MEK inhibitor U0126 on progesterone-induced GVBD. (A) Control oocytes were incubated in ND medium containing 1/1000 DMSO (open circles). U0126-inhibited oocytes were incubated in ND medium containing 10 (black circle), 25 (open square), or 50 μM U0126 (black square). 1 h after U0126 addition, oocytes were stimulated with progesterone. White spots were scored every hour and GVBD was assessed by dissection of oocytes. (B) Western blot analysis. At the end of treatment (20 h), 5 oocytes were taken off, homogenized and immunoblotted with antibodies against $p39^{Mos}$, $Xp42^{Mpk1}$, phospho-MEK, and $p90^{Rsk}$.

meiotic resumption) was 1.5 ± 0.2 fold of $GVBD_{50}$ of control oocytes treated with DMSO. By contrast, in oocytes treated with U0126 50 μM, time of $GVBD_{50}$ was 1.8 ± 0.1 fold of control oocytes. This difference may suggest that the effects of U0126 may be dose-dependent. In support of this, a logrank test showed heterogeneity between GVBD kinetics in DMSO, U0126 10, 20, and 50 μM ($P < 0.05$, $n = 4$).

The preceding results suggest that MAPK activity is dispensable for GVBD in *Xenopus* oocytes. To confirm this, we examined the effects of U0126 upon $p39^{Mos}$ accumulation as well as the phosphorylation status of $Xp42^{Mpk1}$ and its downstream target $p90^{Rsk}$ by Western blotting at the end of each experiment (20 h post-progesterone; Fig. 1B). In immature oocytes (Fig 1B, first lane) $p39^{Mos}$ was not detectable and $Xp42^{Mpk1}$ and $p90^{Rsk}$ were unphosphorylated. In control oocytes treated with DMSO and stimulated with progesterone (second lane), $p39^{Mos}$ was present and $Xp42^{Mpk1}$ and $p90^{Rsk}$ were phosphorylated. By contrast, $Xp42^{Mpk1}$ and $p90^{Rsk}$ phosphorylation were only partially inhibited in oocytes treated with 10 μM U0126 and progesterone, whereas they were totally inhibited in U0126 25-μM- and 50-μM-treated oocytes. However, U0126 treatment up to 50 μM never abolished $p39^{Mos}$ accumulation but resulted in a slight decrease of the detected amounts (Fig. 1B). Phosphorylation of MEK1 was never inhibited even if concentration of U0126 was increased up to 50 μM. This observation agrees with report of Davies et al. (2000), which demonstrated that U0126 blocks $Xp42^{Mpk1}$ phosphorylation through direct inhibition of phosphorylated MEK1 and not by preventing phosphorylation of MEK1. As we already showed in insulin-treated oocytes (Baert et al., 2003), U0126 incubation partially inhibited Raf phosphorylation in progesterone-stimulated oocytes (Fig. 5, lane 7). These results show that MAPK activity is indeed dispensable for GVBD in *Xenopus* oocytes.

Interestingly, though inhibition of MAPK activation did not prevent GVBD, it did significantly inhibit white-spot formation. The percentage of control (DMSO-treated) oocytes with white spots was 93.1% ± 3.6 compared with 66% ± 9.8, 58.7% ± 9.1, and 58.1% ± 8.8 of oocytes treated with 10, 25, or 50 μM U0126, respectively. Decreased white-spot formation was not a reflection of delayed progression through meiosis as the rate of white-spot formation in U0126-treated oocytes did not increase beyond these levels for at least 20 h after progesterone treatment. These results suggest that inhibition of MAPK activation somehow interferes with anchoring of the meiotic spindle at the cortex.

Effects of $p39^{Mos}$ morpholinos antisense on G2/M transition induced by hormonal stimulation

The effects of U0126 upon GVBD may be attributed to non-specific effects on different signaling pathways. To control for this, we used alternative strategies to inhibit the $p39^{Mos}$–$Xp42^{Mpk1}$ pathway. Previously, we have reported that injection of antisense phosphorothioate oligonucleotides of $p39^{Mos}$ ($p39^{Mos}$ PSAS) not only prevented activation of the $p39^{Mos}$–$Xp42^{Mpk1}$ pathway but also delayed GVBD (Baert et al., 2003). Here, we report similar effects with antisense Morpholino oligonucleotides ($p39^{Mos}$-MAS) against $p39^{Mos}$ synthesis on progesterone-stimulated oocytes (Fig. 2A). Injection of 1 ng of sense Morpholinos oligonucleotides ($p39^{Mos}$-MS) of $p39^{Mos}$ had no effect on maturation time course: time of $GVBD_{50}$ was 1.0 ± 0.1 fold those of control oocytes injected with water. In contrast, the time of $GVBD_{50}$ of $p39^{Mos}$-MAS-injected oocytes was increased by 1.4 ± 0.1 fold.

To confirm that these oligonucleotides prevented $p39^{Mos}$ synthesis, we used Western blotting to examine their effects on the $p39^{Mos}$–$Xp42^{Mpk1}$ pathway (Fig. 2B). $p39^{Mos}$ was detected in neither immature oocytes nor $p39^{Mos}$-MAS-injected oocytes. As expected, lack of $p39^{Mos}$ synthesis resulted in abolition of $Xp42^{Mpk1}$ and $p90^{Rsk}$ activation as demonstrated by their lack of phosphorylation (Fig. 2B). Our results showed that, like $p39^{Mos}$-PSAS, $p39^{Mos}$-MAS prevents $p39^{Mos}$ synthesis, MEK1 phosphorylation, and $Xp42^{Mpk1}$ activation (Fig. 2B) and causes a delay in GVBD. Thus, both phosphorothioate and Morpholinos strategies can be used as alternative strategies to prevent activation of the $p39^{Mos}$–$Xp42^{Mpk1}$ pathway.

Blocking $p39^{Mos}$ synthesis or inhibition of MEK1 alters bipolar spindle morphogenesis and induces aster-like formation following progesterone stimulation

Our observation that white-spot formation was inhibited by U0126 suggested that MAPK inhibition interfered with meiotic spindle anchoring at the cortex. Curiously, $p39^{Mos}$-MAS injection had little or no effect on white-spot formation (Fig. 2A). In progesterone-stimulated oocytes, $p39^{Mos}$-MAS injection resulted in 82.0% ± 7.3 of white spot compared to 85.5% ± 3.3 in water-injected oocytes and 75.6% ± 8.6 in $p39^{Mos}$-MS-injected oocytes. To investigate this further, we performed cytological and immunocytological analyses on progesterone and insulin-stimulated oocytes that had been treated with either U0126 or $p39^{Mos}$-antisense oligonucleotides. These analyses were performed 2 h after stabilization of white-spot percentage. Control DMSO-treated oocytes stimulated by progesterone exhibited meiotic spindles at the cortex with condensed chromosomes on a metaphase plate in 93.0% ± 5.0 of oocytes examined (Table 1; Figs. 3F–H) and spindle formation was slightly decreased in control oocytes injected with $p39^{Mos}$-PSS (82.0% ± 1.1 bipolar spindle; Table 1 and Figs. 3L–N). Similarly, although the proportion of oocytes with bipolar spindles were lower in control $p39^{Mos}$-MS-injected oocytes, there was no significant difference in regard to cytological structures found in $p39^{Mos}$-MS-injected versus control H_2O-injected oocytes (58.0 ± 7.1and 73.2 ± 5.7%, respectively; Table 1). Similarly, there was no significant difference between H_2O and $p39^{Mos}$-PSS-injected oocytes ($n = 5$). By contrast, inhibition of the $p39^{Mos}$–$Xp42^{Mpk1}$ pathway using antisense oligonucleotides

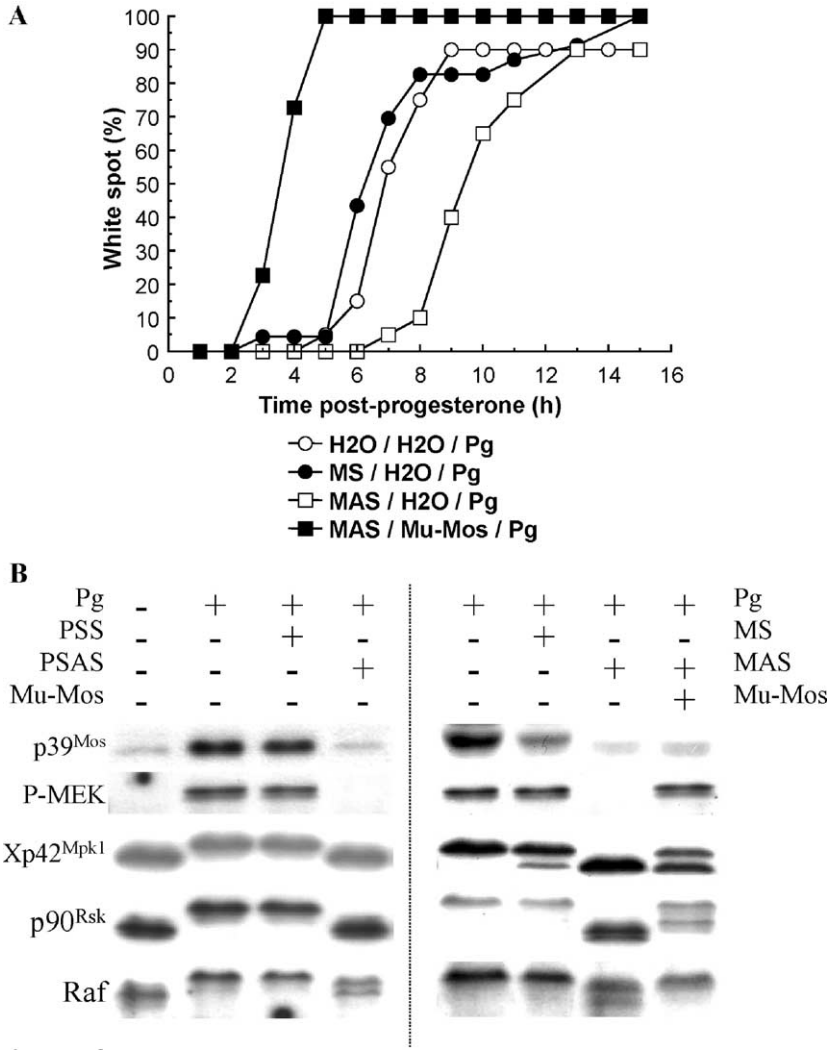

Fig. 2. p39^{Mos} accumulation, MEK1 phosphorylation, Xp42^{Mpk1} and p90^{Rsk} activation, and Raf full phosphorylation are prevented by p39^{Mos} antisense oligonucleotides in progesterone-stimulated oocytes. (A) Control oocytes were micro-injected with water (H_2O/pg; open circles) or p39^{Mos}-sense Morpholinos oligonucleotides (MS/pg; black circles). A batch of oocytes was micro-injected with p39^{Mos}-antisense Morpholinos oligonucleotides (MAS/pg; open squares). Murine Mos (Mu-Mos) has also been injected in MAS-injected oocytes (MAS/Mu-Mos/pg; black squares). After overnight incubation, oocytes were stimulated by progesterone. Appearance of white spot was monitored every 30 min and GVBD was assessed by dissection of oocytes. (B) Western blot analysis was performed either on Morpholinos and Phosphorothioate Oligonucleotide-injected oocytes. At the end of treatment (16 h), 5 oocytes were taken off, homogenized and immunoblotted with antibodies against p39^{Mos}, phospho-MEK, Xp42^{Mpk1}, p90^{Rsk}, and Raf. Murine Mos (Mu-Mos) injection restored Raf and MEK1 phosphorylation but did only partially restore Xp42^{Mpk1} and p90^{Rsk} levels of phosphorylation.

or U0126 resulted in a significant decrease in bipolar spindle formation (Table 1; Figs. 3R, S and 4J, K). Bipolar meiotic metaphase spindles were observed in only 17.0% ± 7.2 of the oocytes treated with 50 μM U0126, in 10.0% ± 10.0 of oocytes injected with p39^{Mos}-PSAS and in 3.8% ± 3.8 of oocytes injected with p39^{Mos}-MAS (Table 1). Statistical analysis confirmed that there was a significant difference between DMSO and U0126 50 μM-treated oocytes, between p39^{Mos}-MS and p39^{Mos}-MAS-injected oocytes and between p39^{Mos}-PSS and p39^{Mos}-PSAS-injected oocytes (each $P < 0.001$, $n = 3$).

The percentage of bipolar spindles observed in U0126-treated oocytes decreased in a dose-dependent manner (Table 1; Fig. 3R): whereas 41.0% ± 19.5 of 10 μM U0126-treated oocytes exhibited a bipolar spindle, only 9.2% ± 5.8 of 25 μM U0126-treated oocytes did (Table 1; Fig. 3R). If we failed to detect bipolar spindles in these oocytes, we observed aster-like structures (Table 1; Fig. 3R). The formation of aster-like structures in U0126-treated oocytes appeared to be dose-dependent (Table 1; Fig 3R); 10 μM U0126 induced aster formation in 17.9% ± 17.9 of oocytes whereas 50 μM U0126 led to the formation of aster-like structures in 61.2 ± 9.3 of oocytes ($P<0.05$).

Similar to U0126-treated oocytes, aster-like structures were found in 76.0% ± 10.8 of the oocytes injected with p39^{Mos}-PSAS (Table 1; Figs. 3O–Q and 4K) and 78.7% ± 2.9 of the oocytes injected with p39^{Mos}-MAS (Table 1; Figs. 3E and 4B, K). In comparison, aster-like structures were detected only in 1.8% ± 1.8 of the control oocytes treated with 0.1% DMSO, in 14% ± 3.6 of oocytes injected with

Table 1
Effects of U0126, p39^{Mos}-MAS, and PSAS oligonucleotides on spindle morphogenesis following progesterone-induced maturation

Treatment	Number of oocytes (number of females)	Metaphase spindle	Aster	No structure
DMSO/pg	56 (3)	52	1	3
U0126 10 μM/pg	28 (3)	12	7	9
U0126 25 μM/pg	23 (3)	2	6	15
U0126 50 μM/pg	54 (7)	9	31	14
U0126 50 μM/Mu-Mos/pg	18 (2)	2	10	6
U0126 50 μM/CA-Rsk/pg	33 (3)	23	5	5
H_2O/pg	34 (3)	25	2	7
MS /pg	33 (5)	18	5	10
MAS/pg	36 (4)	2	30	4
MAS/Mu-Mos/pg	73 (5)	46	16	11
PSS/pg	53 (5)	46	7	0
PSAS/pg	40 (5)	3	31	6
PSAS/Mu-Mos/pg	25 (2)	18	4	3
PSAS/CA-Rsk/pg	35 (3)	6	10	19

This table includes bipolar spindle morphogenesis rescue experiments by Mu-Mos, CA-Rsk injection in absence of MAP kinase pathway activation (pg: progesterone; MS: p39^{Mos}-sense morpholino oligonucleotides; MAS: p39^{Mos}-antisense morpholino oligonucleotides; PSS: p39^{Mos}-sense phosphorothioate oligonucleotides; PSAS: p39^{Mos}-antisense phosphorothioate oligonucleotides).

p39^{Mos}-PSS and in 10.2% ± 4.5 of the oocytes injected with p39^{Mos}-MS (Table 1).

Upon further confirmation of these results, we noted that the extrusion of the first polar body was also impaired by inhibition of the p39^{Mos}–Xp42^{Mpk1} pathway. Detection of the polar body can be accurately performed on 7 μm sections: polar bodies have distinctive shape from remaining follicular cells and are located between the plasma membrane and the vitelline membrane in a V-shaped depression (Figs. 3C and 4A). Though first polar bodies were found in 68.7% ± 3.3 of DMSO-incubated oocytes, they were never detected in U0126-treated oocytes, whatever the concentration was. While 10 μM U0126 did not totally block Xp42^{Mpk1} phosphorylation as shown in Fig. 1B, this partial inhibition was sufficient to prevent polar body extrusion. Similarly, polar bodies were not detected in p39^{Mos}-MAS-injected oocytes.

To confirm the presence of condensed chromosomes in association with these aster-like structures, we performed immunofluorescent staining using Hoechst and antibodies directed against tubulin on sections of cold methanol-fixed oocytes. We observed condensed chromosomes that had undergone diakinesis associated with microtubules both in U0126-treated (Figs. 3I–K) and p39^{Mos}-antisense-injected oocytes (Figs. 3O–Q). Interestingly, where condensed chromosomes were observed, we noted that the signal appeared weaker than in metaphase II control oocytes. One might argue that the aster-like structure could be interpreted as a polar view of a misorientated metaphase spindle in the cytoplasm. However, this is unlikely, since, on such a polar view, we would not expect to observe nucleated microtubules radiating around an aggregate of chromosomes. The aster-like structures observed were always larger than metaphase spindles (i.e., in 50 μM U0126-treated oocytes, aster-shaped microtubular structures observed are 2.0 ± 0.5 fold larger than control metaphase II spindle; also compare Figs. 3H and N with K and Q) and were never located at the cortex but rather were observed in the subcortical cytoplasm. Indeed, in p39^{Mos}-PSAS-treated oocytes, microtubular structures were found at the plasma membrane in only 33.3% ± 8.3 of the oocytes but in 86% ± 3.6 of the cases in p39^{Mos}-PSS-injected oocytes. Similarly, structures were found in subcortical area in 58.3 ± 8.3 and even in deep cytoplasm in 8.3% ± 8.3 of p39^{Mos}-PSAS-injected oocytes. By contrast, in p39^{Mos}-PSS-treated oocytes, structures were observed in subcortical area in 5.5% ± 5.5 of the cases and in deep cytoplasm in 6.7% ± 6.7 of the oocytes.

Collectively, these results establish that inhibition of the p39^{Mos}–Xp42^{Mpk1} pathway by either a small-molecule inhibitor or p39^{Mos}-antisense strategies prevents spindle formation, not by preventing microtubule nucleation but by blocking establishment of a bipolar axis.

CA-Rsk injection does not rescue spindle organization in p39^{Mos} antisense-injected oocytes

To confirm the requirement for the p39^{Mos}–Xp42^{Mpk1} pathway in bipolar spindle formation, rescue experiments were performed using Mu-Mos or CA-Rsk, a downstream substrate of MAPK (Figs. 4 and 5). We observed that while Mu-Mos injection rescued the establishment of a bipolar spindle in 65.7% ± 4.2 of p39^{Mos}-MAS-injected oocytes (n=5; Table 1; Figs. 4C and K) and in 75% of p39^{Mos}-PSAS-injected oocytes (n=2; Table 1 and Fig. 4K), the injection of CA-Rsk failed to properly rescue normal spindle morphogenesis in p39^{Mos}-PSAS-injected oocytes (19 ± 13.2, n=3; Table 1 and Figs. 4D–F and K). We determined that there were no significant differences between control oocytes injected with p39^{Mos}-PSS and oocytes co-injected with Mu-Mos and p39^{Mos}-PSAS, as well as between control oocytes injected with p39^{Mos}-MS and oocytes co-injected with Mu-Mos and p39^{Mos}-MAS.

Consistent with its role as an upstream activator of MEK1, we observed that Mu-Mos was not able to restore a metaphase spindle at the cortex in U0126-treated oocytes (12.5% metaphase spindle vs. 57.5% aster; Table 1 and Fig. 4J). However, CA-Rsk injection at the same concentration as was used in antisense-injected oocytes rescued normal bipolar spindle in 74.9% ± 12.6 of U0126-treated oocytes (Table 1; Figs. 4G–I and J). These results indicate that inhibition of bipolar spindle formation is a specific consequence of MAP kinase pathway inhibition.

Discussion

Taken together, our results obtained using p39^{Mos} antisense strategies and chemical inhibitors of MEK as well

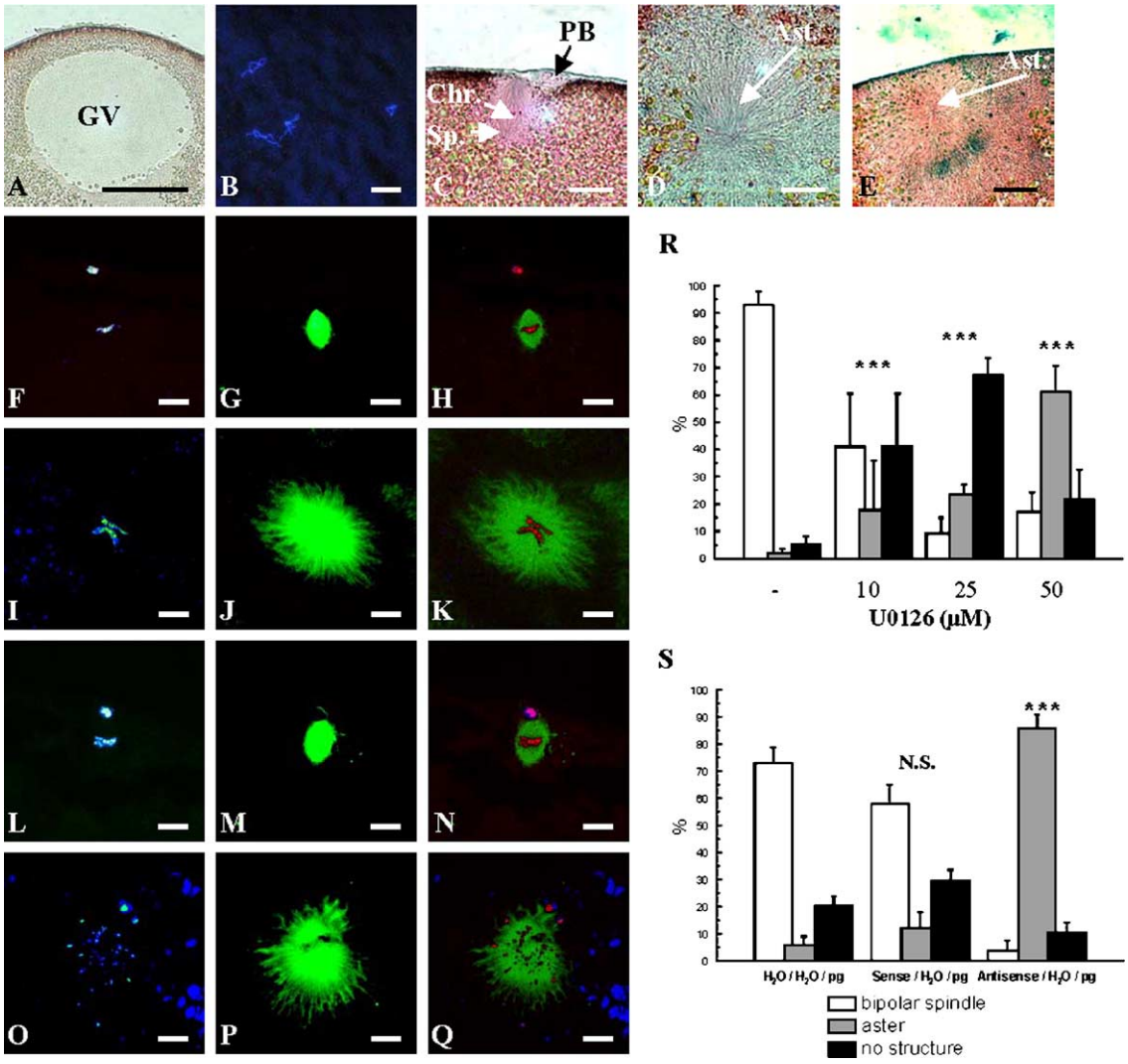

Fig. 3. Effects of U0126 or p39^{Mos}-antisense oligonucleotides on spindle morphogenesis during progesterone-induced maturation. (A–B) Immature non-treated oocytes. (A) Germinal vesicle (nuclear red/picro-indigocarmine staining). (B) Chromosomes decondensed at prophase I (Hoechst staining). (C) Metaphase II-arrested oocyte exhibits typical bipolar spindle with chromosomes and the first polar body (nuclear red/picro-indigocarmine staining). (D) Typical aster-shaped microtubular structure of a U0126-treated oocyte. (E) Typical aster-shaped microtubular structure of an antisense-injected oocyte. (F–H) Typical bipolar spindle with chromosomes of a control oocyte treated with DMSO 1/1000 and then incubated in progesterone. Polar body remained at vitelline membrane, which was separated from the plasma membrane because of oocyte's sections. (F) Hoechst staining. (G) Anti-tubulin staining of the same figure as panel F. (H) Merging of panels F and G. (I–K) Typical aster-shaped microtubular structure with chromosomes of an oocyte treated with 50 μM U0126 and then incubated in presence of progesterone. (I) Hoechst staining. (J) Anti-tubulin staining of the same figure as panel I. (K) Merging of panels I and J. (L–N) Typical bipolar spindle with chromosomes of a control oocyte injected with p39^{Mos} sense oligonucleotides and then incubated in progesterone. (L) Hoechst staining. (M) Anti-tubulin staining of the same figure as panel L. (N) Merging of panels L and M. (O–Q) Typical aster-shaped microtubular structure with chromosomes of an oocyte treated with p39^{Mos} antisense oligonucleotides and then incubated in presence of progesterone. (O) Hoechst staining. (P) Anti-tubulin staining of the same figure as panel O. (Q) Merging of panels O and P. Scale bars represent 15 μm except for panel A where scale bar represents 250 μm. Ast.: aster-shaped microtubular structure, Chr.: chromosomes, PB: polar body, Sp.: bipolar spindle, GV: germinal vesicle. (R) Histogram showing percentages of the different structure types observed in oocytes treated with DMSO or with 10, 25, or 50 μM U0126 and then incubated in presence of progesterone. Error bars represent SEM values. Significance toward DMSO/progesterone treatment is indicated. (S) Histogram showing percentages of the different structure types observed in oocytes treated with water (H_2O), p39^{Mos}-sense oligonucleotides (sense), or p39^{Mos}-antisense oligonucleotides (antisense) and then incubated in presence of progesterone. White bars show percentages of normal bipolar spindles, gray bars show percentages of aster-shaped microtubular structures and black bars show percentages of oocytes lacking any microtubular structures. Error bars represent SEM values. Significance toward water/progesterone treatment is indicated. N.S.: nonsignificant ($P > 0.05$); *significant ($P < 0.05$); **very significant ($P < 0.01$); ***highly significant ($P < 0.001$).

as those of others have established that GVBD can occur in absence of p39^{Mos} accumulation or Xp42^{Mpk1} activity (Baert et al., 2003; Bodart et al., 2002; Dupre et al., 2002; Gross et al., 2000). In these conditions, GVBD and MPF activation are delayed in comparison to control oocytes. However, we observed that egg cytoplasm-induced GVBD was delayed in p39^{Mos}-AS-injected oocytes, whereas it was not in U0126-treated oocytes, suggesting that p39^{Mos} may play a role independently of Xp42^{Mpk1} and p90^{Rsk} in control of meiosis dynamic (Sellier and Bodart, personal

observations). This effect could be mediated by the $p39^{Mos}$ capacity to directly phosphorylate Myt1 independently of $p90^{Rsk}$ (Peter et al., 2002) or to promote protein synthesis through mos response element (de Moor and Richter, 1997).

In contrast to mouse, the involvement of the MAP kinase pathway in spindle morphogenesis in *Xenopus* oocytes in vivo has not been extensively studied. Studies have shown that in vitro MAPK inhibition leads to half spindle formation (Horne and Guadagno, 2003). In accordance with previous reports, we failed to observe meiotic structures at the cortex of oocytes either treated with U0126 (Bodart et al., 2002; Gross et al., 2000) or injected with $p39^{Mos}$-antisense Morpholinos oligonucleotides (Dupre et al., 2002). Instead, we observed the formation of an aster-like structure in the cytoplasm in absence of MAPK activity. Kotani and Yamashita (2002) have reported the absence of

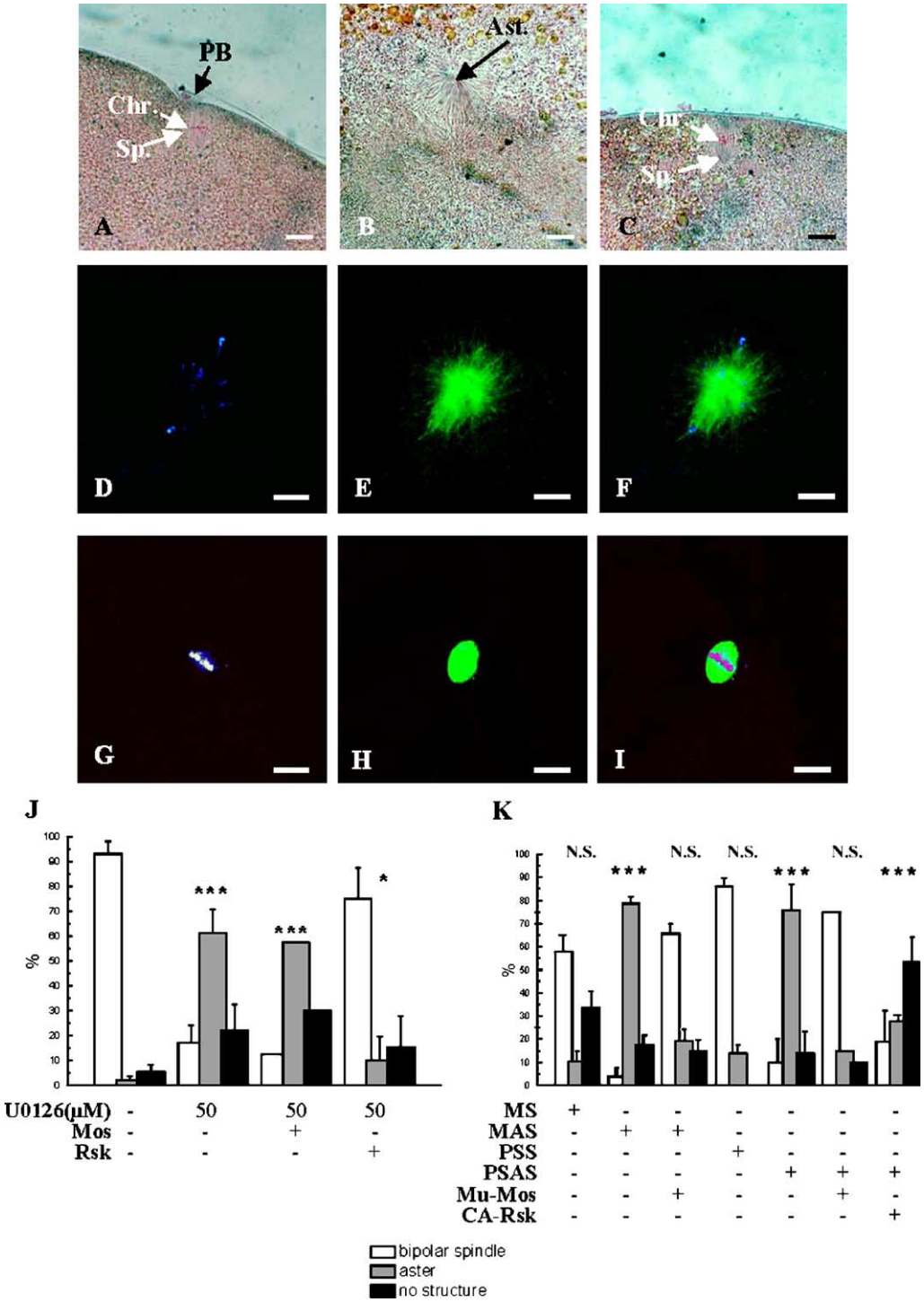

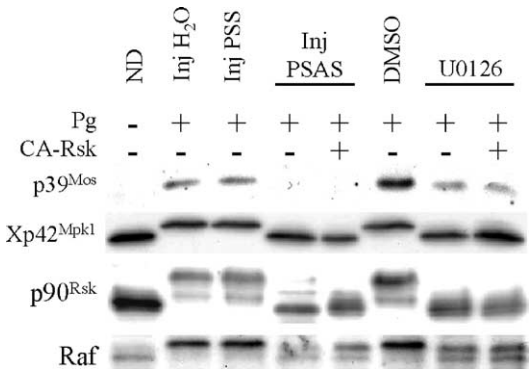

Fig. 5. Effects of p39^{Mos}-antisense oligonucleotides and CA-Rsk injections in progesterone-stimulated oocytes. Western blot analysis. Homogenized oocytes were immunodetected with antibodies against p39^{Mos}, phospho-MEK, Xp42^{Mpk1}, p90^{Rsk}, and Raf. Constitutively active Rsk (CA-Rsk) injections did not restore the activation of any of the p39^{Mos}–MEK1–Xp42^{Mpk1} cascade nor affected Raf level of phosphorylation.

Table 2
Requirement of members of the p39^{Mos}–Mek1–Xp42^{Mpk1}–p90^{Rsk} pathway in meiotic spindle morphogenesis in *Xenopus* oocytes

Treatment	Mos	Xp42^{Mpk1}	Rsk	Structure observed
S/DMSO	Y	Y	Y	Spindle
U0126	Y	N	N	Aster
U0126/Mu-Mos	Y	N	N	Aster
U0126/CA-Rsk	Y	N	Y	Spindle
p39^{Mos}-AS	N	N	N	Aster
p39^{Mos}-AS/CA-Rsk	N	N	Y	No structure
p39^{Mos}-AS/Mu-Mos	Y	Y	Y	Spindle

S: p39^{Mos}-sense oligonucleotides injection; p39^{Mos}-AS: p39^{Mos}-antisense oligonucleotides injection; Mu-Mos: murine Mos injection; CA-Rsk: constitutively active Rsk injection; Y stands for active status of protein as assessed by the phosphorylation status of the protein itself or for its downstream target; N stands for the absence of activation or presence of the considered protein.
Maturation is stimulated by progesterone.

MTOC organization, chromosome condensation, and bipolar formation in U0126-treated *Rana japonica* oocytes. In U0126-treated oocytes, they observed a partial condensation followed by re-condensation of chromosomes together with a dispersed pattern of microtubules. In contrast to these observations, we have observed microtubule nucleation in *Xenopus* oocytes either treated with U0126 or injected with p39^{Mos}-AS oligonucleotides. These asters were associated together with chromosomes that have undergone diakinesis. DNA replication and cell cycling in *Xenopus* oocytes, observed when MAPK pathway is inhibited (Dupre et al., 2002; Gross et al., 2000), might account for the absence of microtubule nucleation and chromosome condensation observed in about 20% of treated oocytes.

MAP kinase pathway is also clearly dispensable for GVBD to occur in mouse oocytes (Abrieu et al., 2001; Colledge et al., 1994; Hashimoto et al., 1994). In Mos-nullizygous mice, oocytes still exhibited spindle morphogenesis but spindle shape was altered and such spindle did not migrate toward the plasma membrane. This leads to an asymmetric division together with the extrusion of an abnormally large polar body (Verlhac et al., 2000). However, polar body extrusion was neither observed in p39^{Mos}-AS-injected nor in U0126-treated oocytes in which Xp42^{Mpk1} phosphorylation was only partially inhibited. Absence of migration of GV content and microtubule toward the plasma membrane, as well as yolk platelet surroundings, may have prevented any polar body extrusion. Role of p39^{Mos} in cytostatic activity (CSF), which maintains high levels of MPF activity in metaphase II-arrested oocytes through the prevention of cyclin B degradation, is mediated by Xp42^{Mpk1} (Abrieu et al., 1996; Haccard et al., 1993; Minshull et al., 1994) and p90^{Rsk} (Bhatt and Ferrell, 1999; Gross et al., 1999). Meiotic spindle defects were rescued in p39^{Mos}-antisense-injected oocytes by the injection of Mu-Mos, indicating that the activation of the p39^{Mos}–MEK1–Xp42^{Mpk1}–p90^{Rsk} cascade was specifically involved in the establishment of the bipolar axis of meiotic spindle. We have also observed that presence of endogenous p39^{Mos} in U0126-treated oocytes, which was still able to phosphorylate MEK1, or injection of Mu-Mos failed to rescue bipolar spindle formation in these conditions, suggesting that p39^{Mos} is not sufficient on its own to

Fig. 4. Rescue of bipolar spindle morphogenesis in absence of MAP kinase pathway activation by Mu-Mos, MEK, or Rsk injection. (A) Metaphase spindle as observed in oocytes injected with 10 ng sense oligonucleotides and stimulated by progesterone after overnight incubation. (B) Aster-shaped microtubular structure as observed in oocytes injected with 10 ng antisense oligonucleotides against p39^{Mos} synthesis and stimulated by progesterone after overnight incubation. (C) Bipolar spindle with chromosomes as observed in oocytes injected with 10 ng antisense oligonucleotides against p39^{Mos} synthesis, incubated overnight and then injected with constitutively active murine Mos before progesterone treatment. (D–F) Typical aster-shaped microtubular structure with chromosomes as observed in oocytes injected with p39^{Mos} antisense oligonucleotides, incubated overnight and then injected with constitutively active Rsk prior to progesterone treatment. (E) Hoechst staining. (F) Anti-tubulin staining of the same figure as panel E. (G) Merge of panels E and F. (G–I) Typical bipolar spindle with chromosomes as observed in oocytes treated with 50 μM U0126, incubated 1 h and injected with constitutively active Rsk before progesterone stimulation. (H) Hoechst staining. (I) Anti-tubulin staining of the same figure as panel H. (J) Merging of panels H and I. (J) CA-Rsk but not murine Mos restored spindle formation in U0126-treated oocytes; histogram showing percentages of the different structure types observed in oocytes incubated stimulated with progesterone in presence of DMSO, 50 μM U0126, or 50 μM U0126 and injected with either constitutively active Mos or Rsk. Error bars represent SEM values. Significance toward DMSO/progesterone treatment is indicated. (K) Murine Mos but not CA-Rsk rescued bipolar axis establishment in AS-injected oocytes: histogram showing percentages of the different structure types observed in oocytes treated with p39^{Mos}-sense Morpholino oligonucleotides (MS), p39^{Mos}-antisense Morpholino oligonucleotides (MAS), p39^{Mos}-sense phosphorothioates oligonucleotides (PSS), or p39^{Mos}-antisense phosphorothioates oligo-nucleotides (PSAS) and rescue capacity of murine Mos and constitutively active Rsk injection into oocytes treated either with p39^{Mos}-antisense oligonucleotides (MAS or PSAS) and then incubated in presence of progesterone. White bars show percentages of normal bipolar spindles, gray bars show percentages of aster-shaped microtubular structures, and black bars show percentages of oocytes lacking any microtubular structures. Error bars represent SEM values. Significance toward water injection/progesterone treatment is indicated: N.S.: nonsignificant ($P > 0.05$); *significant ($P < 0.05$); **very significant ($P < 0.01$); ***highly significant ($P < 0.001$).

enable spindle organization. Injection of CA-Rsk was sufficient to rescue the formation of a bipolar spindle at the plasma membrane in U0126-treated oocytes (Table 2). This supports a crucial role for $p90^{Rsk}$ in spindle morphogenesis, through its activation by $p39^{Mos}$–MEK1–$Xp42^{Mpk1}$ cascade. If injection of CA-Rsk was able to rescue spindle morphogenesis in U0126-treated oocytes, it was not in $p39^{Mos}$-antisense-injected oocytes (Table 2). Failure of spindle restoration in $p39^{Mos}$-PSAS and CA-Rsk co-injected oocytes, as well as in U0126-treated oocytes exhibiting $p39^{Mos}$ levels sufficient to induce MEK1 phosphorylation, suggests that $p39^{Mos}$ and $p90^{Rsk}$ are not sufficient on their own to enable spindle organization. It also suggests that both proteins are required together for spindle morphogenesis and that $p39^{Mos}$ may promote spindle organization through separate pathways.

$p39^{Mos}$ has been demonstrated to associate and phosphorylate tubulin (Zhou et al., 1991). Kinetochores motor protein CENP-E has been demonstrated to exhibit epitopes that are modified upon a Mos-dependent manner in mouse oocytes (Duesbery et al., 1997). Two-hybrid screening leads to the identification of MISS, a MAPK Interacting and Spindle Stabilizing protein. The latter accumulated only in MII, where it was localized to the spindle (Lefebvre et al., 2002). DOC1R has also been shown to be regulated by phosphorylation during meiotic maturation by MAPK pathway. DOC1R is localized to microtubules and injection of DOC1R antisense RNA leads to microtubule defects in MII oocytes (Terret et al., 2003). Recently, experiments achieved by Gard and colleagues (Becker et al., 2003) have provided new insights in the mechanisms of spindle assembly and microtubule organization in *Xenopus* oocytes: while NuMA and dynein are required for the organization of TMA (Transient microtubule array) and MTOC, XMAP215 and kinesin-related XKCM1 have antagonistic roles in the regulation of microtubule assembly and organization. Nevertheless, further analyses are required to determine how $p39^{Mos}$ and its downstream effectors could regulate the molecular mechanisms of spindle morphogenesis. Because we did observe aster-like structure similar to those observed following progesterone stimulation in either XMAP215 antibodies or XKCM1 antibodies injected oocytes (Becker et al., 2003), one might hypothesize that these molecules could be targeted by the $p39^{Mos}$–$Xp42^{Mpk1}$ pathway.

Our work provides in ovo evidence that the $p39^{Mos}$–MEK1–$Xp42^{Mpk1}$–$p90^{Rsk}$ cascade is required for correct establishment of bipolar axis of the meiotic spindle in *Xenopus* oocytes.

Acknowledgments

We thank Arlette Lescuyer-Rousseau for technical assistance. We are grateful to Pr A. 'Vauban' Leprêtre for statistical analysis. We also thank Dr. Vande Woude and Dr. Nebreda for murine Mos and CA-Rsk, and for helpful discussions. This work was supported by grants from the French "Ministère de l'Education Nationale" (UPRES-EA 1033) and from the "Association pour la Recherche sur le Cancer".

References

Abrieu, A., Lorca, T., Labbe, J.C., Morin, N., Keyse, S., Doree, M., 1996. MAP kinase does not inactivate, but rather prevents the cyclin degradation pathway from being turned on in *Xenopus* egg extracts. J. Cell Sci. 109 (Pt. 1), 239–246.

Abrieu, A., Doree, M., Fisher, D., 2001. The interplay between cyclin-B-Cdc2 kinase (MPF) and MAP kinase during maturation of oocytes. J. Cell Sci. 114, 257–267.

Araki, K., Naito, K., Haraguchi, S., Suzuki, R., Yokoyama, M., Inoue, M., Aizawa, S., Toyoda, Y., Sato, E., 1996. Meiotic abnormalities of c-mos knockout mouse oocytes: activation after first meiosis or entrance into third meiotic metaphase. Biol. Reprod. 55, 1315–1324.

Azzi, L., Meijer, L., Ostvold, A.C., Lew, J., Wang, J.H., 1994. Purification of a 15-kDa cdk4- and cdk5-binding protein. J. Biol. Chem. 269, 13279–13288.

Baert, F., Bodart, J.F., Bocquet-Muchembled, B., Lescuyer-Rousseau, A., Vilain, J.P., 2003. Xp42(Mpk1) activation is not required for germinal vesicle breakdown but for Raf complete phosphorylation in insulin-stimulated *Xenopus* oocytes. J. Biol. Chem. 278, 49714–49720.

Becker, B.E., Romney, S.J., Gard, D.L., 2003. XMAP215, XKCM1, NuMA, and cytoplasmic dynein are required for the assembly and organization of the transient microtubule array during the maturation of *Xenopus* oocytes. Dev. Biol. 261, 488–505.

Bhatt, R.R., Ferrell Jr., J.E., 1999. The protein kinase p90 rsk as an essential mediator of cytostatic factor activity. Science 286, 1362–1365.

Bodart, J.F., Bechard, D., Bertout, M., Gannon, J., Rousseau, A., Vilain, J.P., Flament, S., 1999. Activation of *Xenopus* eggs by the kinase inhibitor 6-DMAP suggests a differential regulation of cyclin B and p39(mos) proteolysis. Exp. Cell Res. 253, 413–421.

Bodart, J.F., Gutierrez, D.V., Nebreda, A.R., Buckner, B.D., Resau, J.R., Duesbery, N.S., 2002. Characterization of MPF and MAPK activities during meiotic maturation of *Xenopus tropicalis* oocytes. Dev. Biol. 245, 348–361.

Choi, T., Rulong, S., Resau, J., Fukasawa, K., Matten, W., Kuriyama, R., Mansour, S., Ahn, N., Vande Woude, G.F., 1996. Mos/mitogen-activated protein kinase can induce early meiotic phenotypes in the absence of maturation-promoting factor: a novel system for analyzing spindle formation during meiosis I. Proc. Natl. Acad. Sci. U. S. A. 93, 4730–4735.

Colledge, W.H., Carlton, M.B., Udy, G.B., Evans, M.J., 1994. Disruption of c-mos causes parthenogenetic development of unfertilized mouse eggs. Nature 370, 65–68.

Davies, S.P., Reddy, H., Caivano, M., Cohen, P., 2000. Specificity and mechanism of action of some commonly used protein kinase inhibitors. Biochem. J. 351, 95–105.

de Moor, C.H., Richter, J.D., 1997. The Mos pathway regulates cytoplasmic polyadenylation in *Xenopus* oocytes. Mol. Cell Biol. 17, 6419–6426.

Duesbery, N.S., Choi, T., Brown, K.D., Wood, K.W., Resau, J., Fukasawa, K., Cleveland, D.W., Vande Woude, G.F., 1997. CENP-E is an essential kinetochore motor in maturing oocytes and is masked during mos-dependent, cell cycle arrest at metaphase II. Proc. Natl. Acad. Sci. U. S. A. 94, 9165–9170.

Dumont, J.N., 1972. Oogenesis in *Xenopus laevis* (Daudin): I. Stages of oocyte development in laboratory maintained animals. J. Morphol. 136, 153–179.

Dupre, A., Jessus, C., Ozon, R., Haccard, O., 2002. Mos is not required for the initiation of meiotic maturation in *Xenopus* oocytes. EMBO J. 21, 4026–4036.

Fan, H.Y., Tong, C., Lian, L., Li, S.W., Gao, W.X., Cheng, Y., Chen, D.Y., Schatten, H., Sun, Q.Y., 2003. Characterization of ribosomal S6 protein kinase p90rsk during meiotic maturation and fertilization in pig oocytes: mitogen-activated protein kinase-associated activation and localization. Biol. Reprod. 68, 968–977.

Ferrell Jr., J.E., Wu, M., Gerhart, J.C., Martin, G.S., 1991. Cell cycle tyrosine phosphorylation of p34cdc2 and a microtubule-associated protein kinase homolog in *Xenopus* oocytes and eggs. Mol. Cell Biol. 11, 1965–1971.

Fisher, D.L., Brassac, T., Galas, S., Doree, M., 1999 (Oct.). Dissociation of MAP kinase activation and MPF activation in hormone-stimulated maturation of Xenopus oocytes. Development 126 (20), 4537–4546.

Frank-Vaillant, M., Jessus, C., Ozon, R., Maller, J.L., Haccard, O., 1999. Two distinct mechanisms control the accumulation of cyclin B1 and Mos in *Xenopus* oocytes in response to progesterone. Mol. Biol. Cell 10, 3279–3288.

Furuno, N., Nishizawa, M., Okazaki, K., Tanaka, H., Iwashita, J., Nakajo, N., Ogawa, Y., Sagata, N., 1994. Suppression of DNA replication via Mos function during meiotic divisions in *Xenopus* oocytes. EMBO J. 13, 2399–4410.

Gard, D.L., Affleck, D., Error, B.M., 1995. Microtubule organization, acetylation, and nucleation in *Xenopus laevis* oocytes: II. A developmental transition in microtubule organization during early diplotene. Dev. Biol. 168, 189–201.

Gross, S.D., Schwab, M.S., Lewellyn, A.L., Maller, J.L., 1999. Induction of metaphase arrest in cleaving *Xenopus* embryos by the protein kinase p90Rsk. Science 286, 1365–1367.

Gross, S.D., Schwab, M.S., Taieb, F.E., Lewellyn, A.L., Qian, Y.W., Maller, J.L., 2000. The critical role of the MAP kinase pathway in meiosis II in *Xenopus* oocytes is mediated by p90(Rsk). Curr. Biol. 10, 430–438.

Haccard, O., Sarcevic, B., Lewellyn, A., Hartley, R., Roy, L., Izumi, T., Erikson, E., Maller, J.L., 1993. Induction of metaphase arrest in cleaving *Xenopus* embryos by MAP kinase. Science 262, 1262–1265.

Hashimoto, N., Watanabe, N., Furuta, Y., Tamemoto, H., Sagata, N., Yokoyama, M., Okazaki, K., Nagayoshi, M., Takeda, N., Ikawa, Y., et al., 1994. Parthenogenetic activation of oocytes in c-mos-deficient mice. Nature 370, 68–71.

Hatch, K.R., Capco, D.G., 2001. Colocalization of CaM KII and MAP kinase on architectural elements of the mouse egg: potentiation of MAP kinase activity by CaM KII. Mol. Reprod. Dev. 58, 69–77.

Hausen, P., Riebesell, M., 1991. The Early Development of *Xenopus laevis*. Springer Verlag.

Horne, M.M., Guadagno, T.M., 2003. A requirement for MAP kinase in the assembly and maintenance of the mitotic spindle. J. Cell Biol. 161, 1021–1028.

Howard, E.L., Charlesworth, A., Welk, J., MacNicol, A.M., 1999. The mitogen-activated protein kinase signaling pathway stimulates mos mRNA cytoplasmic polyadenylation during *Xenopus* oocyte maturation. Mol. Cell. Biol. 19, 1990–1999.

Kotani, T., Yamashita, M., 2002. Discrimination of the roles of MPF and MAP kinase in morphological changes that occur during oocyte maturation. Dev. Biol. 252, 271–286.

Lee, J., Miyano, T., Moor, R.M., 2000. Localisation of phosphorylated MAP kinase during the transition from meiosis I to meiosis II in pig oocytes. Zygote 8, 119–125.

Lefebvre, C., Terret, M.E., Djiane, A., Rassinier, P., Maro, B., Verlhac, M.H., 2002. Meiotic spindle stability depends on MAPK-interacting and spindle-stabilizing protein (MISS), a new MAPK substrate. J. Cell Biol. 157, 603–613.

Masui, Y., 2001. From oocyte maturation to the in vitro cell cycle: the history of discoveries of Maturation-Promoting Factor (MPF) and Cytostatic Factor (CSF). Differentiation 69, 1–17.

Minshull, J., Sun, H., Tonks, N.K., Murray, A.W., 1994. A MAP kinase-dependent spindle assembly checkpoint in *Xenopus* egg extracts. Cell 79, 475–486.

Nebreda, A.R., Hunt, T., 1993. The c-mos proto-oncogene protein kinase turns on and maintains the activity of MAP kinase, but not MPF, in cell-free extracts of *Xenopus* oocytes and eggs. EMBO J. 12, 1979–1986.

Nurse, P., Masui, Y., Hartwell, L., 1998. Understanding the cell cycle. Nat. Med. 4, 1103–1106.

Perdiguero, E., Pillaire, M.J., Bodart, J.F., Hennersdorf, F., Frodin, M., Duesbery, N.S., Alonso, G., Nebreda, A.R., 2003. Xp38gamma/SAPK3 promotes meiotic G(2)/M transition in *Xenopus* oocytes and activates Cdc25C. EMBO J. 22, 5746–5756.

Peter, M., Labbe, J.C., Doree, M., Mandart, E., 2002. A new role for Mos in *Xenopus* oocyte maturation: targeting Myt1 independently of MAPK. Development 129, 2129–2139.

Sagata, N., Oskarsson, M., Copeland, T., Brumbaugh, J., Vande Woude, G.F., 1988. Function of c-mos proto-oncogene product in meiotic maturation in *Xenopus* oocytes. Nature 335, 519–525.

Terret, M.E., Lefebvre, C., Djiane, A., Rassinier, P., Moreau, J., Maro, B., Verlhac, M.H., 2003. DOC1R: a MAP kinase substrate that control microtubule organization of metaphase II mouse oocytes. Development 130, 5169–5177.

Verlhac, M.H., Kubiak, J.Z., Clarke, H.J., Maro, B., 1994. Microtubule and chromatin behavior follow MAP kinase activity but not MPF activity during meiosis in mouse oocytes. Development 120, 1017–1025.

Verlhac, M.H., Lefebvre, C., Guillaud, P., Rassinier, P., Maro, B., 2000. Asymmetric division in mouse oocytes: with or without Mos. Curr. Biol. 10, 1303–1306.

Zhao, X., Singh, B., Batten, B.E., 1991. The role of c-mos proto-oncoprotein in mammalian meiotic maturation. Oncogene 6, 43–49.

Zhou, R.P., Oskarsson, M., Paules, R.S., Schulz, N., Cleveland, D., Vande Woude, G.F., 1991. Ability of the c-mos product to associate with and phosphorylate tubulin. Science 251, 671–675.